MASSIVE BOULDERS SHIFTED ALONG THE COAST OF GUANTÁNAMO, CUBA, DURING HURRICANE MATTHEW (2016)

Max Engel, Felipe Matos Pupo, Zadiérik Hernández Ortega and Dominik Brill

With 9 figures and 1 table
Received 11 February 2025 · Accepted 7 August 2025

Summary: Hurricane Matthew struck the province of Guantánamo in southeastern Cuba in 2016 by making landfall as the first and only hurricane reaching category 4 in documented history. We surveyed transport path, distance and mode of coastal boulder deposits (CBD) after the event at three coastal sites and compared them with the pre-Matthew boulderscape, which reflects the effects of extreme-wave events on millennial time scales. The application of a dimensionless analytical framework comparing elevation, CBD size and wave climate with a global dataset of storm-transported CBD shows that boulder transport during Matthew is at the uppermost possible limit, while larger boulders that remained inactive hint to even more intense hurricanes or a large tsunami in the prehistoric past. Most observations support typical patterns of storm-transported CBD in carbonate environments, such as a source at the cliff edge, preferential sourcing and clustering at shoreline indentations and a stepwise movement inland during multiple storm events. The study shows that Hurricane Matthew is not unique in Guantánamo in terms of intensity on larger, prehistoric time scales. At the same time, recurrence intervals of highest-category hurricanes in this region may decrease with ongoing climate change prompting the need to use the inland distribution of CBD plus additional buffer as minimum setback zones in coastal hazard management.

Keywords: Coastal boulder deposits (CBD), huracanolitos, coastal geomorphology, cliff erosion, hurricane, tsunami, palaeoclimatology, Greater Antilles, Cuba, tropics, Quaternary geology

1 Introduction

Severe tropical cyclones in the Atlantic basin – referred to as hurricanes (sustained winds >118 km h^{-1}, separated into five categories on the Saffir-Simpson Hurricane Wind Scale, Kelman 2013) – impose substantial hazards of coastal flooding and wind damage to the Caribbean, Gulf of Mexico and the southwest of the US (e.g. Vanselow et al. 2007, de Beurs et al. 2019). The island states of the Caribbean suffer in particular, as (i) annual frequency, lifetimes and intensities of hurricanes have increased in the North Atlantic over recent decades (Emanuel 2005, Mann et al. 2009, Kossin et al. 2020, Vosper et al. 2020) and (ii) these island states are heavily dependent on climate-sensitive economic sectors (Mycoo 2018). Furthermore, it is expected that the frequency of hurricanes and the length of the hurricane season in the Caribbean basin will increase with ongoing global warming (Bustos & Torres 2021).

Even though in eastern Cuba hurricane landfalls are slightly less frequent compared with Western Cuba, the Virgin Islands or the northern Lesser Antilles (Reading 1990, Andrews 2007), they are the most important natural hazard Cuba needs to prepare for (Roura-Pérez et al. 2018, Matos Pupo et al. 2023a). There is an estimate of only four hurricanes of category 5 making landfall in Cuba since 1791, i.e. the storm of San Francisco de Borja in 1846, a hurricane in 1924, the hurricane of Santa Cruz del Sur in 1932 and Hurricane Irma in 2017 (Matos Pupo et al. 2022, Dunán-Avila et al. 2025). None of them, however, reached Guantánamo province (Fig. 1, Fig. 2a), which has only experienced one hurricane landfall of category ≥4 since 1791, i.e. Hurricane Matthew in 2016 (Pérez et al. 2001, Dunan-Avila et al. 2025). This comparably low frequency led to a generally low level of (i) awareness and preparedness, especially before 2016/2017 and in the province of Guantánamo, where immediate personal experiences of major hurricanes were infrequent (Mitrani Arenal 2006, Beltrán-Fonseca 2019, Pérez & Milanés 2020, Matos Pupo et al. 2023a), and of (ii) adaptation measures due to low risk perception of coastal flooding associated with major hurricanes (Matos Pupo et al. 2022).

Given the large return intervals of the strongest hurricanes, which in general may be in the order of hundreds of years (Elsner et al. 2008, May et al. 2013), geological traces of coastal flooding can be instrumental to support regional assessment of coastal hazards and the identification of flood-

https://doi.org/10.3112/erdkunde.2025.03.02 ISSN 2702-5985 (Online)

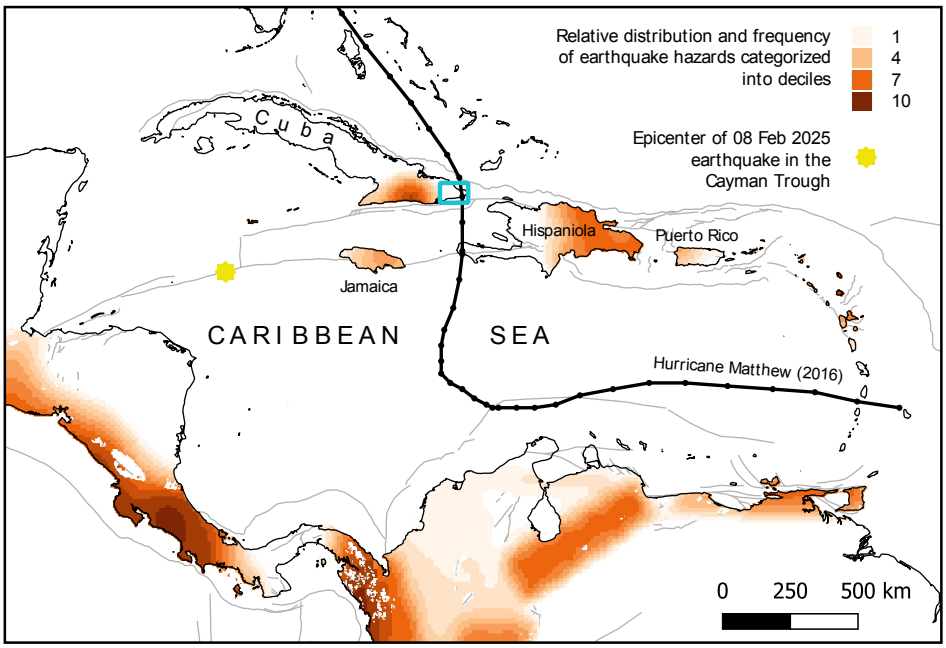

Fig. 1: Overview of the Caribbean basin with the study area in southeastern Cuba (light blue frame, see also Fig. 2a). The map shows the distribution of active faults (grey lines) (Styron 2019), the relative earthquake frequency (CHRR/CIESIN 2005) and the epicenter of the recent M7.6 earthquake of 09 February 2025 to emphasise the regional tsunami hazard. The thick black line shows the track of Hurricane Matthew (thick black line), the dots show 6-hr intervals of hurricane passage based on NOAA NHC Best Track Data HURDAT2 (Landsea & Franklin 2013).

prone areas (Nott 1997, May et al. 2013, Engel et al. 2016, Muller et al. 2017). Large boulders distributed along rocky coasts – coastal boulder deposits (CBD) – with sizes indicating transport only by the most extreme waves, i.e. those from severe storm waves and tsunamis, are excellent recorders in this regard (Paris et al. 2011, Autret et al. 2016, Engel et al. 2016, Cox et al. 2020, Kelletat et al. 2020, Lau & Autret 2020). They help to assess the long-term flooding hazard, map the inland extent of flood-prone areas along the coast (Miller et al. 2014, Engel et al. 2016) and support the quantification of hydrodynamic parametres of coastal flooding through inverse modeling (Nott 1997, Nandasena 2020, Watanabe et al. 2023). However, the most common approaches using initiation-of-motion criteria (e.g. Nott 1997, Engel & May 2012, Miller et al. 2014, May et al. 2015, Lau et al. 2018, Boesl et al. 2020, Nandasena 2020, Nandasena et al. 2014, 2022, Pedoja et al. 2023, Dunán-Avila et al. 2025) contain a number of flaws (Cox et al. 2020, Kennedy et al. 2021) due to substantial gaps in the proper understanding of how CBD are transported by waves and the exact influence of the physical environment (Oetjen et al. 2020). The northern Caribbean has witnessed a quite substantial amount of CBD research providing evidence for long-term extremes of coastal inundation (e.g., Jones & Hunter 1992, Kelletat et al. 2004, Miller et al. 2014, Atwater et al. 2017, Rovere et al. 2017). In Cuba, research on CBD is in its infancy, with a country-wide overview recently presented by Matos Pupo et al. (2023b) and further regional and local studies (Iturralde-Vinent 2017, Rodríguez & Acosta 2017, Beltrán-Fonseca 2019, Rojas-Consuegra et al. 2019, Pedoja et al. 2023, Dunán-Avila et al. 2025).

In order to unlock the value of the boulder record for hazard assessment in the eastern part of Cuba, we mapped coastal boulder transport during category-4 Hurricane Matthew in 2016 at key sites close to its landfall during a post-event survey. While other researchers used this case to test inverse modelling approaches of boulder transport by integrating wave data of the event and characteristics of individual transported boulders at sites in southeastern Cuba (Dunán-Avila et al. 2025), our aim is to document the environmental context of transported and non-transported boulders, their sizes and inland extent. We aim at assessing whether this event was the maximum possible intensity that storms may reach in the region on millennial time scales by comparison of the volume and size of the transported boulders with the pre-event coastal boulderscape. We also evaluate whether strong tsu-

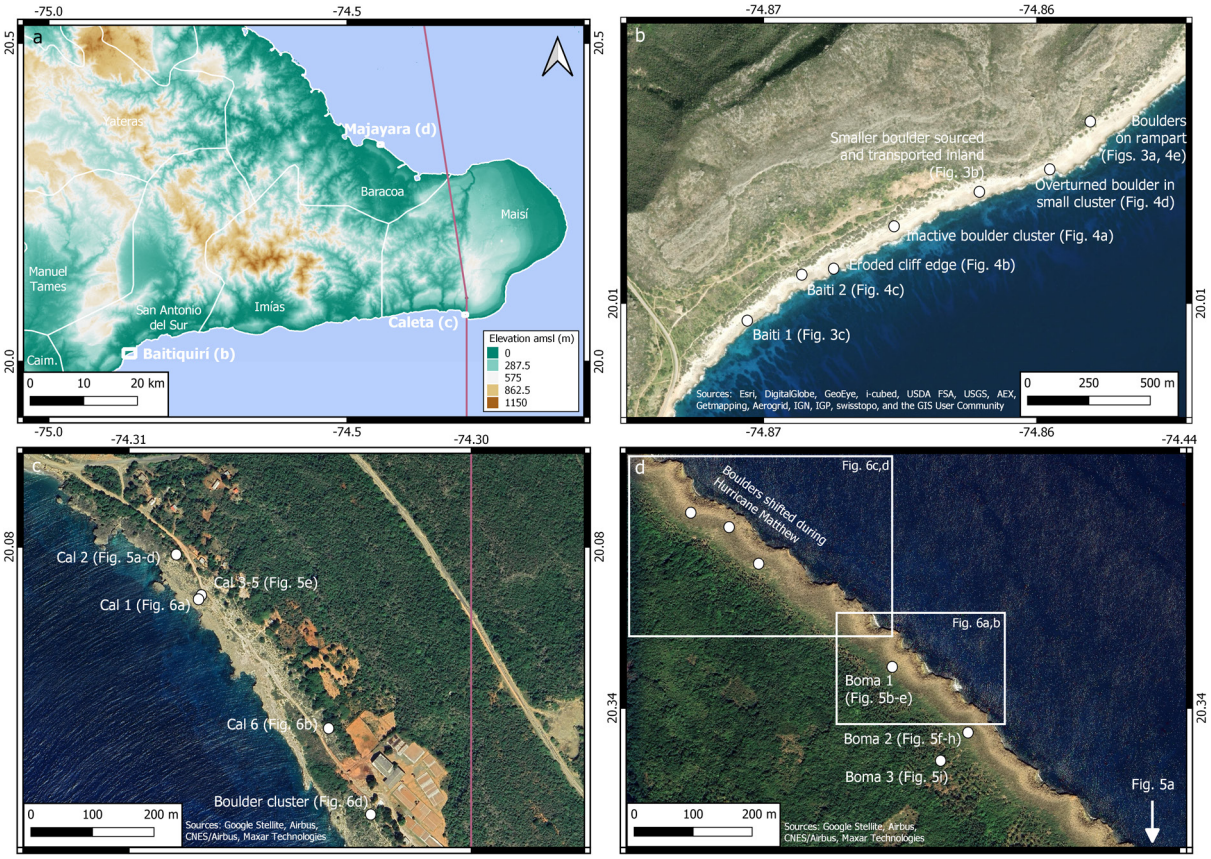

Fig. 2: a) Overview of eastern Cuba (see also light blue frame in Fig. 1) based on ASTER GDEM 2 (product of METI Japan and NASA) with the three survey sites and the track of Hurricane Matthew in 2016 (NOAA NHC Best Track Data HURDAT2 (Landsea & Franklin 2013)). White frames indicate the extent of the detail maps of the surveyed sites (amsl=above mean sea level). b) Baitiquirí, c) Caleta and d) Majayara with the boulders and other geomorphic features presented and discussed in this paper. White frames indicate the location of maps in Fig. 8.

namis have to be taken into account by comparing the CBD with other recent storm records of CBD transport at a global scale through dimensionless analysis.

2 Hurricane Matthew

Starting as a tropical wave on 23 September 2016 off the coast of West Africa, Hurricane Matthew moved westward and developed into a tropical storm on 28 September 2016 when passing Barbados to the north (Stewart 2017). Matthew intensified very quickly to reach category 5 on 30 September, reaching one-minute sustained winds of 140 kt (72 m s^{-1}) on 1 October, remaining at category 4–5 for 102 hours in total (Klotzbach 2017). Matthew made landfall on the Tiburon Peninsula of Haïti on 04 October and later on that day traversed the eastern tip of Guantánamo province in Cuba (Fig. 1, Fig. 2a,c), where the sites of the survey reported here are located, as a category-4 system. It provided 400–500 mm of rain during the passage before moving north towards the Bahamas archipelago (De Beurs et al. 2019).

3 Physical setting

3.1 Study area

Guantánamo is the easternmost of Cuba's provinces, comprising ten municipalities, six of which are prone to coastal flooding: Niceto Pérez, Caimanera, San Antonio del Sur, Imías, Maisí and Baracoa (Gómez et al. 2011). Similar to the entire southeastern coast of Cuba, the south coast of Guntánamo presents the narrowest platform of the Cuban territory, which is exposed to southern winds. Strong winds from migrating anticyclones interacting with extratropical lows are infrequent (mostly occurring around the municipality of Baracoa). Thus, occa-

sional tropical storms and hurricanes represent the main meteorological hazard creating coastal flooding through storm surge and waves. The largest episodes of flooding (since 1960) along the south coast were recorded during hurricanes Sandy (2012) and Matthew (2016) (Perigó et al. 2020).

The north coast has a narrow platform and is open to winds from the first quadrant, which favors oceanic waves with a long fetch. Occasional strong swells in this area resulting in coastal wave heights of 4–5 m (up to 8–10 m during exceptional events) are generated by the influence of migrating anticyclones, their interaction with extratropical lows, as well as tropical storms and hurricanes (Perigó et al. 2020). The entire coastline of the municipality of Baracoa, as well as the north of Maisí, is exposed in this stretch. The largest coastal floods (since 1960) in this sector occurred in the city of Baracoa also during recent events (hurricanes Ike in 2008, Matthew in 2016). The mean tidal range along both coasts is about 50 cm (Kjervfe 1981, Servicio Hidrográfico y Geodésico de la República de Cuba 2003), which seems to have not changed significantly over the Holocene (Khan et al. 2017). The highest astronomical tide remains below 1 m (Dunán-Avila et al. 2025).

3.2 Surveyed sites

The field survey in June 2018 focused on three of the most exposed sites along the coast of Guantánamo, two on the south coast (Baitiquirí, municipality of San Antonio del Sur; Caleta, Maisí) and one on the north coast (Majayara, Baracoa). The site of Baitiquirí (referred to as Bate Bate in Dunán-Avila et al. 2025) is located close to the maximum wind radius of Hurricane Matthew, resulting in a storm surge of 3–4 m, estimated wave heights of 6–8 m, and flooding of up to 100 m inland (Stewart 2017). The coast at Baitiquirí (Fig. 2b), east of Guantánamo Bay, consists of a gently inclined palaeo-reef platform as part of the last-interglacial Jaimanitas Formation (Toscano et al. 1999, Muhs et al. 2017), elevated to c. 6 m above mean sea level (msl) close to the cliff and rising up to c. 11 m above msl at the maximum width of the platform c. 230 m inland (Dunán-Avila et al. 2025). The surface is karstified with rock pools forming at the cliff edge, whereas in some places further inland it is covered by coral rubble, mollusk shells and carbonate sand as well as boulders of different sizes, locally known as *huracanolitos*. The cliff is almost vertical with irregular indentations (slightly lower, trough-shaped part of the seaward platform) and a water depth of c. 10 m at the foot of the cliff, reaching down to c. 80 m at a distance of 500 m offshore (Dunán-Avila et al. 2025). The sites of Caleta (Fig. 2c) and Majayara (Fig. 2d), referred to as Bahía de Boma in Dunán-Avila et al. (2025), are also represented by an elevated palaeo-reef platform of the Jaimanitas Formation, with a very similar elevation as at Baitiquirí. This particular geomorphic setting of an elevated last-interglacial carbonate platform is very common of CBD sites in the Caribbean (e.g. Scheffers 2002, Watt et al. 2010, Engel & May 2012, Miller et al. 2014). At Caleta, where Hurricane Matthew made landfall, the platform is more strongly dipping towards the sea and is more overgrown by shrubs and trees, whereas the cliff edge is more curbed and less distinct. The site of Majayara is exposed to the northeast. The platform has an elevation of c. 5 m above msl right at the coast, with a water depth of c. 5 m in front of the cliff (Dunán-Avila et al. 2025). Near Majayara >3 m of storm surge, 4.5–6 m waves and flooding of up to 300–450 m inland was reported during Hurricane Matthew (Stewart 2017). Fringing reefs to attenuate wave impacts before reaching the coast are absent at all sites (Estrada et al. 2023). The relative sea-level (RSL) history is relatively uniform across the Greater Antilles, with c. 11 m below present msl 8 ka BP, c. 5 m below present msl 6 ka BP and a slow, quasi-continuous rise since then derived for Cuba (Khan et al. 2017).

4 Methods

Sites were selected based on literature search, remote sensing and field surveys (later summarized in Matos Pupo et al. 2023b) prior to the joint-survey conducted by all authors in June 2018. At all three sites, the largest boulders were mapped by recording the length of the main axes and distance to the cliff edge using a measuring tape, and the location using a handheld GPS device. Geomorphic signs of recent transport and overturning during Matthew were documented, as well as the potential pre-transport setting. Furthermore, the minimum flooding extent associated with Hurricane Matthew was mapped in the field based on sedimentary indicators.

We apply the dimensionless framework of Kennedy et al. (2021) to compare boulders both shifted and unaffected by Hurricane Matthew in southeast Cuba with the extreme upper end of recent storm-transported boulders worldwide. The

approach is based on data from western Ireland (Clancy et al. 2016, Cox et al. 2018), Brittany in France (Boudière et al. 2013, Accensi & Maisondieu 2015, Autret et al. 2016, 2018), the eastern Visayas in the Philippines (Mori et al. 2014, May et al. 2015, Kennedy et al. 2017), and Okinawa, Japan (Goto et al. 2011). Dimensional analysis is a powerful technique that helps to simplify and generalize complex physical problems by focusing on the fundamental quantities governing the system, such as mass, length, time and other relevant physical dimensions. In hydrodynamics, it is applied to establish empirical equations between governing parameters when the actual processes are highly complex, as in the case of boulder transport by waves. The lack of dimensions also enables comparisons between different datasets (Roberts et al. 2025).

The dimensionless framework of Kennedy et al. (2021) considers boulder size, density, elevation and significant wave height. It is based on the static balance equation to reconstruct minimum flow velocities for motion of an object with a long, intermediate and short axis (a, b, c) on a flat ground surface (Nott 1997, Nandasena 2020), generalized to

$$(1) \qquad \frac{U^2}{gl\left(\frac{\varrho_s}{\varrho_w}-1\right)} = f_1(shape,\ coefficients,\ settings)$$

where U is the depth-averaged flow velocity, g is the gravitational constant, ϱ_s is the density of rock, ϱ_w is the density of seawater (commonly set as 1.02 g cm^{-3}). l is a representative boulder length scale defined as

$$(2) \qquad l = \sqrt[3]{V}$$

where V=volume of the boulder. f_1 (and f_2–f_4) are dimensionless functional relationships of certain properties of the boulders, their transport and their environment, respectively. U^2 can be described as

$$(3) \qquad U^2 = gH_s f_2\left(\frac{Z}{H_s}, \frac{X}{H_s}, topography,\ bathymetry\right),$$

relating flow velocity at the boulder to significant wave height offshore (H_s), elevation above high tide (Z), distance inland from the coastline at high tide (X) and site-specific bathymetry and topography. Equations (1) and (3) give

$$(4) \qquad \frac{H_s}{l\left(\frac{\varrho_s}{\varrho_w}-1\right)} = f_3\left(\frac{Z}{H_s}, \frac{X}{H_s}, topography,\ bathymetry,\ shape,\ coefficients,\ setting\right)$$

where $f_3=f_1/f_2$ and coefficients refer to a wide range of largely unvalidated values chosen for lift and drag forces (Cox et al. 2020, Nandasena 2020). For the very common case of waves approaching a cliff coast and boulders resting on the cliff top, as in the southeast of Cuba, the relationship expressed in (4) can be given as

$$(5) \qquad l^* = \frac{l\left(\frac{\varrho_s}{\varrho_w}-1\right)}{H_s} = f_4\left(\frac{Z}{H_s}, \frac{X}{H_s}, \frac{c}{b}\right).$$

Kennedy et al. (2021) then investigate the size-elevation relationship of the global dataset and simplify by neglecting the parametres inland distance (X/H_s) and shape (c/b) using equation (5). As a result, they calculate a dimensionless space where storm transport is possible, expressed as

$$(6) \qquad \frac{Z}{H_s} = 0.75 l^{*-0.7} tanh^{0.25}\left(\frac{3(l^*_{max}-l^*)}{l^*_{max}}\right)$$

where the limits of the dataset were set to l*=[0,0.9], i.e. l_{max}=0.9, and Z/H_s=2.5 (Kennedy et al. 2021).

For testing the moved and unmoved boulders mapped during the Cuba survey, we apply a H_s of 7.3 m for the south coast (Baitiquirí, Caleta) and 7.4 m for Majayara, which is the maximum offshore value determined during Hurricane Matthew (Dunán-Avila et al. 2025). Boulder-specific parameters were measured during the survey and, in part, confirmed by or adapted from Dunán-Avila et al. (2025).

5 Results

5.1 Field mapping

5.1.1 Baitiquirí

At Baitiquirí (Fig. 2b), numerous boulders are distributed on top of the elevated palaeo-reef platform which has an intensely karstified cliff-edge zone (Fig. 3a,c). Very few of them were quarried at the cliff edge and shifted inland recently (Fig. 3b), probably during Hurricane Matthew, as indicated by edges of light-coloured limestone at the cliff (Fig. 3b,c, Fig. 4b). The largest of these examples is boulder Baiti 1 (Tab. 1, Fig. 3c, Fig. 4b). In fact, it seems that most of the collapsing cliff-edge material drops into the sea and remains in the subtidal in front of the cliff. Only a very small part becomes shifted inland during the abrasional process, exemplified by the large fresh scar and scarcity of correlating boulders in Fig. 4b. Finer-grained overwash deposits of carbonate sand, shell debris and smaller coral fragments were mapped high on the platform, behind a c. 20 m wide sediment-free zone

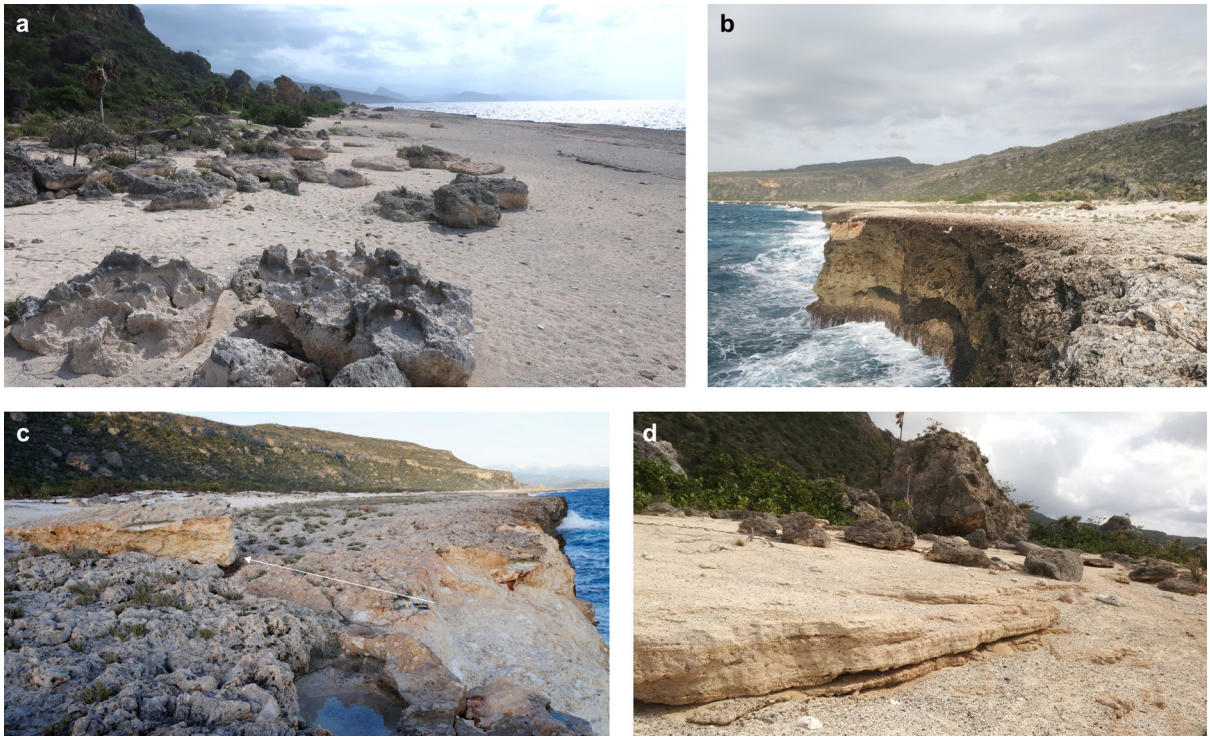

Fig. 3: Baitiquirí plate, Part 1. a) Largest boulder cluster at Baitiquirí, with mainly moderately sized (a-axis c. 1–2 m) slab-shaped boulders, some of which appear imbricated. They are located seaward of a rampart and washover lobe with smaller recently active boulders that reach further inland into the palmtree vegetation (Fig. 4e). Only some of the boulders were sourced from the cliff edge or subtidal and added to the cluster recently based on differences in colour. Light bands with a vertical extent of 20–30 cm at the bottom of the boulders indicate recent net erosion of finer-grained sediment. b) One of several recent erosional scars at the edge of the remarkably vertical cliff at Baitiquirí, with the corresponding smaller boulder transported onto the carbonate platform for ~30 m. c) Boulder Baiti 1 (Tab. 1; a-axis=7.3 m) recently quarried at the cliff edge and transported for a few metres. The white arrow indicates the transport from the light erosional scar at the cliff edge to the current position, possibly during Hurricane Matthew. d) Consolidated and stratified sand- to fine gravel-sized washover deposit on top of the ~6 m-high carbonate platform. The large block in the background is a collapsed part of the landward Jaimanitas Formation.

(Fig. 3a,b,d, Fig. 4a,c). In some places they are lithified in a beachrock-type (or cayrock-type) manner (Fig. 3d), mostly through the influence of sea spray (De Leeuw et al. 2000) as described by several authors for higher supratidal elevations (e.g. Gischler & Lomando 1997, Kelletat 2006). Elsewhere, these deposits bury larger and older boulders which remained unmoved during recent storms (Fig. 4a). They furthermore provide the source for a rampart or berm ridge (*sensu* Otvos 2000) of sand, skeletal debris and boulders further inland – locally referred to as *camellones de tormentas* (Peñalver et al. 2013) –, which is stabilized and overgrown by large shrubs and palmtrees. In one specific place, this rampart was modified, most likely during Hurricane Matthew, through fresh, white sand and boulder components (a-axis up to 1.5 m) colliding with and destroying some long-standing palmtree vegetation at an elevation of c. 7 m above mean sea level c. 30 m inland from the cliff edge (Fig. 4e). No particular indicators of flow depth were mapped at this particular site, thus 7 m above msl is the minimum estimate. Some of the boulders show a very light colouring with a vertical extent of 20–30 cm on their lower part (Fig. 3a, Fig. 4c,d) indicating very recent erosion and redeposition of the fine-grained deposits. Some of the older boulders were overturned during the hurricane indicated by living vegetation pointing downward (Fig. 4d).

The second largest of the few recently shifted boulders is Baiti 2. It is rather flat and seems to have rested on top of the platform before transport, with the lowermost part buried in sediment. As the most seaward boulder of a pre-existing cluster, it was the only one shifted during Hurricane Matthew, possibly supported by high sediment loads of the fluid given the substantial finer-grained deposits covering the karstified platform. It was overturned and shoved onto another unmoved larger boulder of the cluster (Fig. 4c).

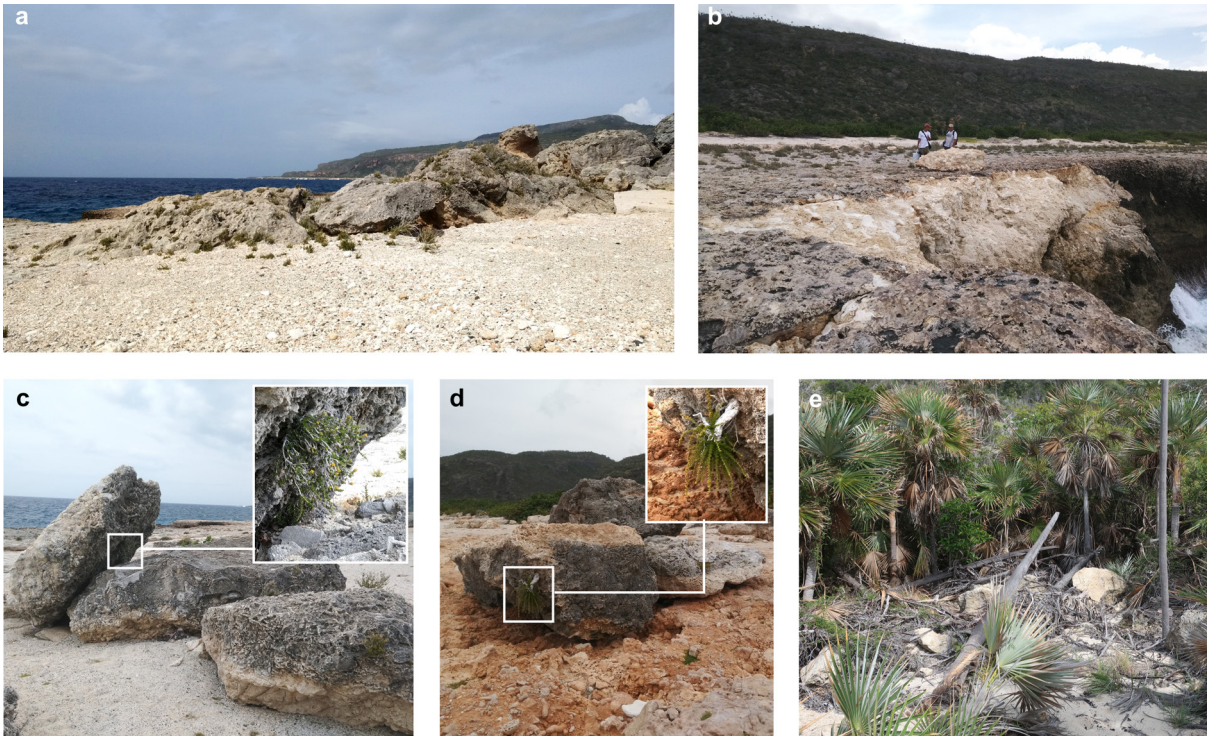

Fig. 4: Baitiquirí plate, Part 2. a) Older, inactive boulders buried in sand to fine gravel-sized washover deposits. The setting indicates recent net accumulation of these washover deposits. b) Large erosional scar at the cliff edge with only one small boulder recently transported onshore, possibly during Hurricane Matthew. c) Boulder Baiti 2 (Tab. 1) on the left was recently transported and shoved onto another boulder, possibly during Hurricane Matthew. The two other boulders were not moved and stripped from 20–30 cm of finer-grained washover deposits based on the white colouring at their bottom. Baiti 2 was overturned based on recent vegetation at the former upper surface. Its pre-transport location was on top of the platform probably close to its current position and at least 20 m away from the cliff edge as the most seaward zone of the platform is entirely free of vegetation. d) Cluster with pre-existing subaerial boulder transported and overturned during Hurricane Matthew based on downward-pointing vegetation, in combination with net erosion of finer-grained deposits (light-coloured underside of unmoved boulder in the background). e) Recent lobe-shaped washover deposit of carbonate sand, shell debris, coral fragments and boulders overprinting the inland rampart, landward of the boulder cluster in Fig. 3a.

5.1.2 Caleta

At Caleta (Fig. 2c), the concentration of boulders on top of the reef-top platform (c. 6 m asl) is higher, and a higher percentage of boulders seems to have been transported recently compared to Baitiquirí. The survey focused on the northern part of the Caleta boulder field. Boulders with main axes of up to 8.0 m (Cal 2) were shifted (Fig. 5a, Fig. 6c,d), while the largest ones at the site, such as Cal 6 further inland, remained inactive (Fig. 6b). The largest boulders show strongly developed karst features in the current setting, such as karst pipes penetrating from the top deep into the boulder, in addition to being heavily overgrown (Fig. 5a,b). The largest recently active boulder, Cal 2, exhibits two rock-pool generations with an inactive bottom tilting in a different angle than the active, horizontal one (Fig. 5c). Some of the large, active rock pools on top of the boulders are filled with white, coarse carbonate sand, testifying to recent flooding and wave action on top of the platform (Fig. 5c). Patches of massive carbonate sand, shell debris and coral fragments cover the karstified surface of the platform in a thickness of up to 50 cm, in some parts showing reddish brown coloring and root penetration as signatures of incipient pedogenesis. This coloring was identified especially around and below Cal 2, where, however, also plastic packaging of unknown age was found incorporated into the reddish brown sand (Fig. 5a,d).

Compared to Baitiquirí, there were fewer light-colored bottom parts of boulders as signature of recent fine-sediment erosion, and also fewer fresh scars at the cliff edge (Fig. 5e). Boulder Cal 1 is the only boulder clearly associated with a fresh erosional scar at the cliff edge, with a transport distance of c. 7 m inside a shoreline indentation or reentrant, respectively (Fig. 6a). A few meters further inland inside the same indentation, a cluster of three larg-

Tab. 1: Boulders mapped during the field survey. For location see Fig. 2. Boulder volume V_{abc} is calculated by multiplying the three axes and an empirical correction factor of 0.54 derived from other limestone boulders in a comparable setting based on structure-from-motion data in Boesl et al. (2020). A correction factor in this range is confirmed by other studies in carbonate boulder settings (e.g. Engel & May 2012, Gienko & Terry 2014, May et al. 2015, Dunán-Avila et al. 2025). V_{SfM} values are from Dunán-Avila et al. (2025). Density values for Baitiquirí after Beltrán-Fonseca (2019), for Majayara after Dunán-Avila et al. (2025). For Caleta the average value between Baitiquirí and Majayara was used; Z=elevation (m); X=distance from the cliff edge (m).

Site	ID	a (m)	b (m)	c (m)	V_{abc} (m^3)	V_{SfM} (m^3)	Density (g cm^{-3})	Mass (t)	Shifted during Matthew?	Transport distance	Z (m above msl)	X (m)	Min. flooding during Hurricane Matthew (m)	Field notes
Baitiquiri	Baiti 1	7.3	3.3	1.7	22.1	25.9	2.59	67.1	Yes	9 m	6	9	>95	Very close to shore, light reddish brown limestone, quarried and moved during Hurricane Matthew (2016)
	Baiti 2	3.8	2.2	1.3	5.9	-	2.59	15.3	Yes	?	6	42		Shifted and overturned, in cluster with two other larger boulders that were inactive during Matthew
Caleta	Cal 1	2.3	1.7	1.0	2.1	-	2.48	5.2	Yes	?	6	7	>80	Subangular; reddish stain on limestone, karstified; overturned → downward oriented plants; close to cluster of older boulders
	Cal 2	8.0	2.8	1.3	15.7	-	2.48	38.9	Yes	Few m	6	33		Pre-Matthew, two rock-pool generations (+ other post-depositional karst features), heavily overgrown, plastic trash in sand partly covering the boulder (with very light pedogenesis); root penetration into the karst cavities; below the boulder dark reddish brown sand, pedogenesis and dense root network
	Cal 3	5.3	3.1	1.5	13.3	-	2.48	33.0	Yes	Few m	6	22		Karstified limestone, Cal 3–5 placed in shoreline indentation
	Cal 4	4.4	2.7	1.2	7.7	-	2.48	19.1	Yes	?	6	17		Closest to the shore within the cluster, tossed on Cal 5
	Cal 5	3.4	1.4	0.6	1.5	-	2.48	3.7	Yes	?	6	20		Elongated
	Cal 6	10.0	3.8	2.0	41.0	-	2.48	101.7	No	-	7	64		Elongated; not overturned, but laterally turned (180°); heavily overgrown and karstified, two rock-pool generations; former surface tilted landward; originates from cliff edge; associated with small, fresh debris indicating flooding during Hurricane Matthew up to this point
Majayara	Boma 1	10.9	4.4	1.1	28.5	31.5	2.37	74.7	Yes	38 m	6.5	38	>50	Quarried from the cliff edge and transported to its current location during Hurricane Matthew; overturned, underside with deep rock pools; bottom roughness extreme, rock pools at current cliff edge of up to more than 1 m depth
	Boma 2	5.9	2.5	1.5	11.9	-	2.37	28.2	Yes	<1 m	6.5	50		Older, grey boulder, shifted marginally during Matthew
	Boma 3	5.9	2.3	1.6	11.7	-	2.37	27.7	No	-	8	105		Heavily overgrown in forest (z4), overturned

er boulders was mapped which show signs of recent transport for a very short distance (Cal 3–5) (Fig. 5e). The largest boulder at the site (Cal 6, a-axis=10.0 m) is located 65 m from the cliff edge and was not recently moved. The a-axis, original aligned with the shoreline, has been laterally turned for 180° at some point, as the former cliff edge and upper part of the intertidal bioerosional notch are now directed inland (Fig. 6b), exposing the largest surface defined by a- and c-axes against the flow. It is heavily overgrown and also features two distinct rock-pool generations at the tilted former surface. In the southern part of the site, more boulders were transported onto the platform possibly from a

Fig. 5: Caleta plate, Part 1. a) Boulder Cal 2, the largest clast at the site with signs of recent movement (a few metres only; Tab. 1). It is located at a distance of 33 m from the shoreline, turned by 180° from its former orientation as part of the cliff edge and rests on a thick finer-grained washover deposit (Fig. 2c). b) Cal 2 shows very deep round karst pipes going through almost the whole boulder indicating long-term subaerial chemical weathering. These karst pipes form after transport inland along pre-defined vertical cracks and indicate a minimum time span of several centuries since initial sourcing and transport. c) The current and long-term surface orientation is different from its original setting as part of the former cliff edge, as indicated by two rock-pool generations, where the tilted rock-pool bottom represents the cliff-edge stage. d) Cal 2 resting on finer-grained washover deposit with recent root penetration and intercalated plastic (insert). e) Overview of the Caleta site with boulders Cal 1 and 3–5 resting in a shoreline indentation. The omnipresent cover of finer-grained washover deposits at the site starting c. 10 m from the cliff edge is clearly visible.

subtidal pre-hurricane setting, based on the whitish colour and a lack of erosional scars at the cliff edge (Fig. 6c,d).

5.1.3 Majayara

Majayara, a site exposed to the northwest, inside the Bahía de Boma, is located c. 9 km west of Hurricane Matthew's track (Figs. 1a,d). Only very few larger boulders were found on the cliff-top platform. In contrast to the other two sites, sheets, lobes or patches of carbonate sand, shell debris and coral fragments are absent on top of the platform (Fig. 7c), either due to a lack of source material in the foreshore or more efficient backwash. The site of Majayara shows a very clear shore-parallel zonation, where the first c. 15 m from the cliff edge are bare, almost black-colored and show the highest degree of karstification (z1). The zone c. 15–35 m from the cliff edge shows low and patchy shrub vegetation (z2), whereas the zone 35–50 m is already densely overgrown (z3). The zone beyond 50 m is dominated by palmtrees and dense undergrowth (z4) (Fig. 7a,i). Most of the few boulders on the platform in z2 and z3 show signs of recent transport, mostly through a very light color (Fig. 7a,c–e,) and based on bitemporal satellite image comparison (cf., Fig. 8). Most are very flat (Fig. 7a,c). Numerous erosional scars are visible at the cliff edge (Fig. 7b, Fig. 8d), even more than at Baitiquirí. The largest boulder Boma 1 (a-axis=10.9 m) was quarried and transported to its current position on top of the carbonate platform by waves of Hurricane Matthew (see also Dunán-Avila et al. 2025). Most of the material eroded during the hurricane, including large boulders comparable to Boma 1, is resting in the foreshore (Figs. 7c–e), as reported by a local diver. Boma 1 is overturned and experienced sliding transport on the platform based on continuous impact marks on the platform (Figs. 7c,e, 8b) and all over the underside of the boulder (former surface of the cliff edge), which is covered by deep rockpools. The a-axis of

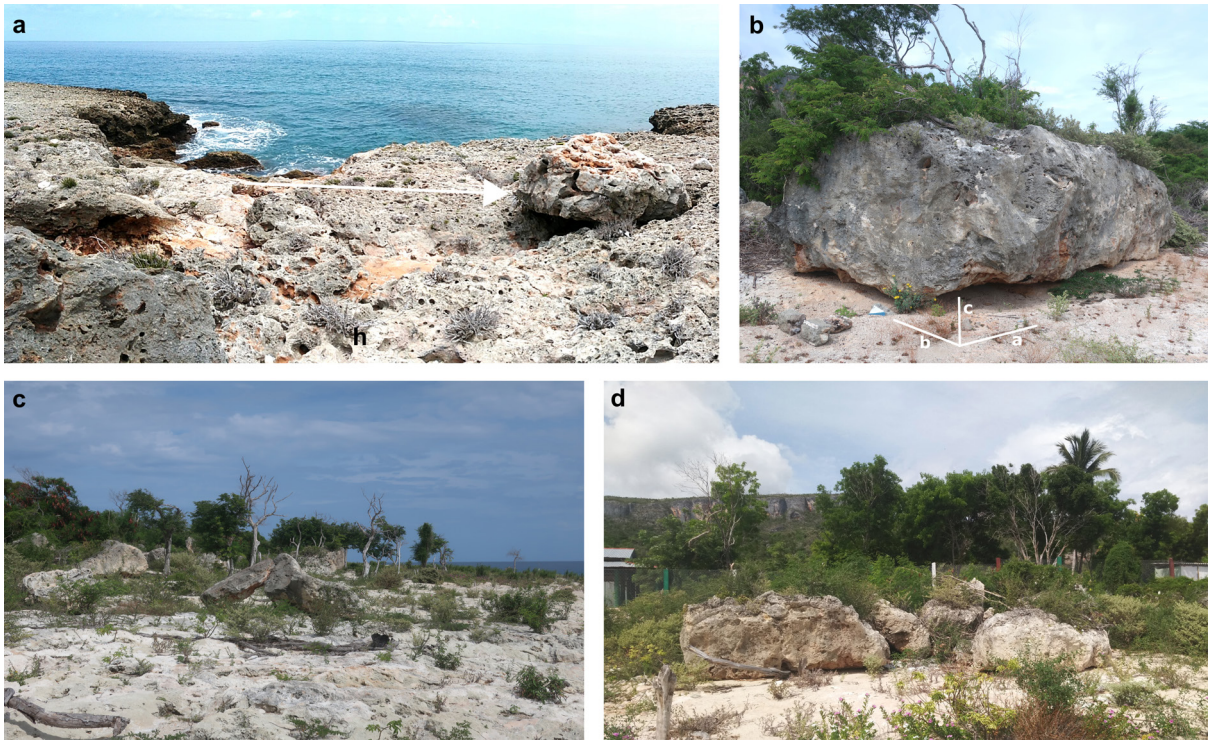

Fig. 6: Caleta plate, Part 2. a) Cal 1 (Tab. 1) in the shoreline indentation on top of the palaeo-reef platform, was sourced at the cliff edge, overturned and transported for c. 7 m. b) Boulder Cal 6 (Tab. 1) is the largest boulder at Caleta (a-axis=10.0 m) and was not recently moved. It is also laterally turned for 180° , i.e. the originally seaward facing cliff edge and upper part of the intertidal notch are now facing inland. The largest projected area defined by a- and c-axes are facing the inland flow on top of the platform. Cal 6 is the only boulder at the site showing some indication of net erosion of finer-grained washover deposits (in the back, on the right). c) Further recently active boulders in the southern part of Caleta. Their delicate placement either indicates synchronous sliding movement with the larger boulder being pushed under the smaller one, or the smaller boulder being pushed onto the larger one by the backwash of waves overtopping the platform. d) Cluster of recently active boulders in the southern part of Caleta based on light colouring and a tree trunk stuck underneath the largest boulder.

10.9 m is aligned perpendicular to the transport direction. The abundance of fresh erosional scars at the cliff edge is in stark contrast to the lack of fresh boulders on the cliff top. Boulder Boma 2 was one of the very few to exist on the platform before Hurricane Matthew, most likely for longer time in the range of decades at least, based on its dark colour (Fig. 7g); it was only shifted for <1 m (Fig. 7f). It shows at least two rock pool generations (Fig. 7h). There seem to be a number of old boulders hidden by dense vegetation in z4 at an elevation of 8 m above msl and up to 100 m inland from the cliff edge, exemplified by boulder Boma 3 (Fig. 7i).

5.2 Dimensionless analysis of size-elevation relationship

Comparing the largest boulders moved by waves of Hurricane Matthews on top of the 6–7 m high terrace of the Jaimanitas Formation to other global size-elevation data of recent storm-transported CBD using the approach of Kennedy et al. (2021) (envelope function of eq. 6) shows Boma 1 and Baiti 1 plotting at the uppermost end of the global distribution (Fig. 9). Depending on the size scale – l (eq. 2) or b-axis –, Boma 1 even plots beyond the function defining what is considered possible during storm transport. The largest boulder documented during the whole survey, Cal 6, resting relatively far inland at Caleta and not shifted during Hurricane Matthew plots beyond the function no matter what size measure is applied.

6 Discussion

6.1 Processes of boulder transport

All three sites show a typical zonation of high-energy tropical rocky coasts with a cliff and elevated carbonate platform. The cliff edge is moderately to heavily karstified, similar to the high-energy coastal model defined by Focke (1978) for Curaçao.

Fig. 7: Majayara plate. a) Overview of the Majayara site with characteristic shore-parallel surface zonation (z1=barren, heavily karstified surface; z2=moderately to heavily karstified surface with isolated small shrubs; z3=moderately karstified surface with dense overgrowth; z4=palm trees with dense undergrowth). The (unnamed) boulder at the z2/z3 boundary was transported onshore during Hurricane Matthew. b) One of many recent erosional scars at the cliff edge attributed to cliff erosion during Hurricane Matthew, with most of the eroded material deposited in the foreshore. This one is in front of boulder Boma 1. c) Boma 1 (Tab. 1) c. 45 m from the cliff edge at the z2/z3 boundary. Continuous fresh scars on top of the platform indicating the recent sliding and/or rolling transport path probably from the cliff edge to its current position. d) Overturned boulder Boma 1 with the extent of its a-axis (10.9 m) and c-axis (1.4 m). e) Erosional scars indicating the transport path of Boma 1. f) Boulder Boma 2 was shifted by <1 m during Hurricane Matthew indicated by light colouring underneath its previous position. g) Boma 2 in z3, close to the boundary with z2, with the extent of its a-axis (5.9 m) and c-axis (1.5 m). h) Two rock-pool generations identified on top of Boma 2, which is turned laterally for 180°. i) Boulder Boma 3 far inland in z4, densely overgrown and without any signs of recent movement.

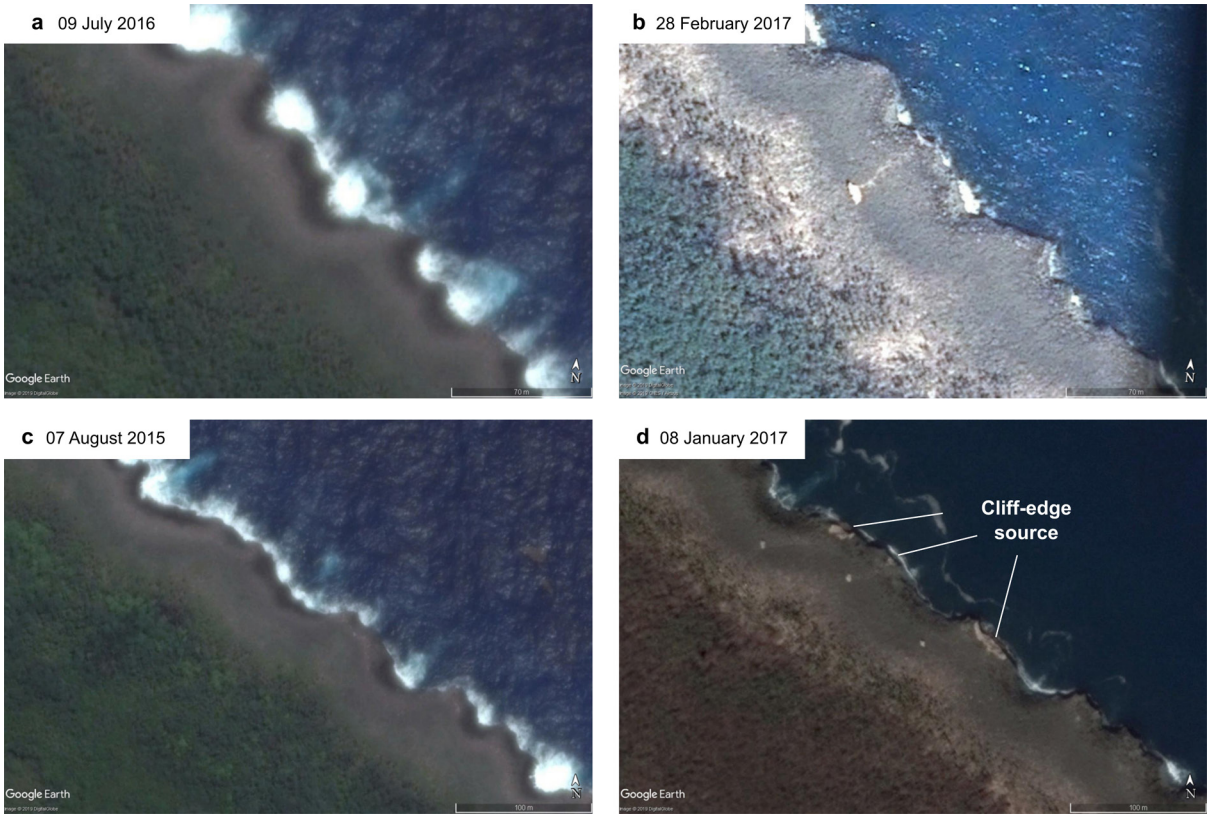

Fig. 8: Pre- and post-Matthew satellite imagery (Google Earth, Digital Globe) at the Majayara site (see Fig. 2d for location of satellite images). a,b) Largest boulder Boma 1 (Fig. 7c). Massive light scars on the limestone surface (see also Fig. 7e) indicate a slightly curving transport path from a submerged pre-transport setting in the foreshore. Slight changes in transport direction show the stepwise transport during the hurricane with slightly shifting approaching angles of waves. c,d) Three individual boulders north of a,b), with scars indicating more oblique transport vectors. Quarry niches are much larger than the boulders showing that the majority of rocks quarried from the cliff edge end up in the foreshore.

The general topography is somewhat higher and steeper, without a well-defined intertidal surf bench constructed of coralline algae and other accretions (rather resembling the low-energy, leeward model of Focke (1978) in this aspect). The cliff edge represents the spray zone, followed by the barren zone (z1 at Majayara), where fine or coarse sediment is either transported landward or washed back into the sea. Vegetation is absent due to recurring overtopping of waves and the strong influence of sea spray. Only exceptionally large boulders such as Baiti 1 may rest here for a short time right after being sourced at the cliff edge, before being transported further inland or back into the sea by the backwash of subsequent major overtopping waves. The barren zone is followed either by a zone of vegetation (z2 at Majayara) or sand, shells and coral debris (Baitiquirí and Caleta), the latter experiencing strong redistribution during major flooding events as indicated by buried boulders and white exposed parts of boulders. The suspended, redistributed sand further may enhance the transport capacity of the overtopping waves on the platform in a way that is not yet entirely understood (Nandasena & Tanaka 2013), which represents an additional factor of uncertainty for inverse hydrodynamic modelling.

Boulder deposits are found from the barren zone (only very recent, large ones) up to the heavily overgrown landward zones further inland (z3, z4 at Majayara). The landward limit of recurring flooding and sediment transport is often marked by ramparts or berm ridges, best developed at Baitiquirí and usually controlled by the availability of sediment material in the foreshore. These represent the finer end of the landward fining pattern of clast distribution, which is the result of long-term sorting by periodic storm activity at boulder sites (Goto et al. 2009, 2010, Cox et al. 2018, Lau & Autret 2020); sometimes the ramparts are overprinted by aeolian processes. Thus, all three sites represent slight variations of the typical setting and zonation of storm-dominated boulder sites at tropical carbonate coasts

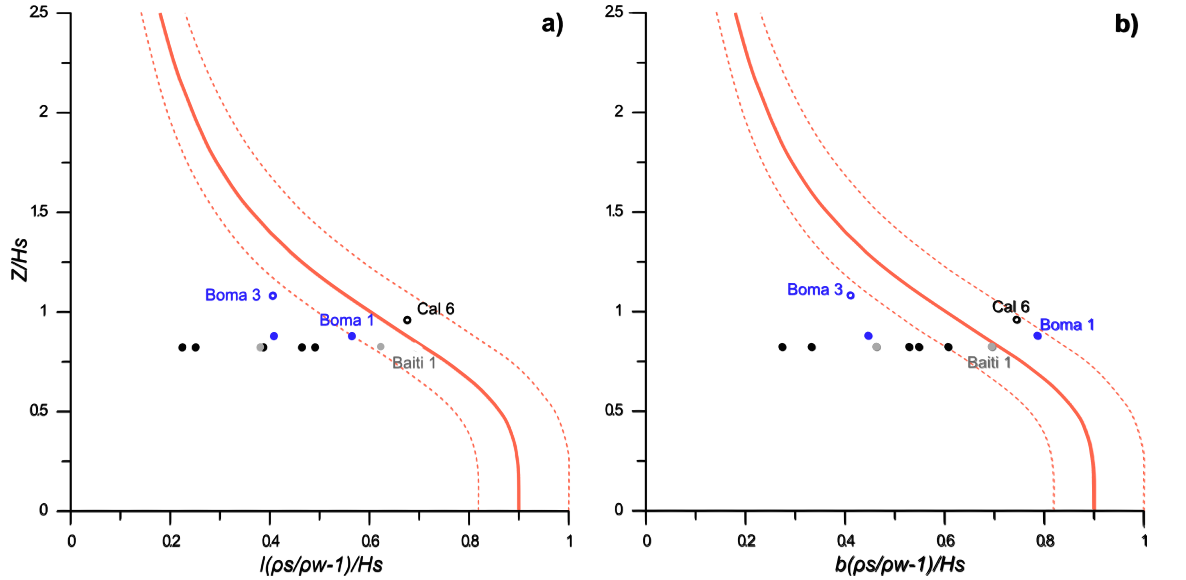

Fig. 9: Dimensionless size-elevation relationship for boulders from Baitiquirí (grey), Caleta (black) and Majayara (blue) either moved (closed circles) or not moved (open circles) during Hurricane Matthew. The two diagrams use different simplified boulder size scales: a)=l (eq. 2); b)=b-axis. The dimensionless parameter space of boulder transport by storms calculated by Kennedy et al. (2021) based on global boulder datasets is shown by the red function (eq. 6).

as e.g., described in detail for the east coast/windward side of Bonaire in the southern Caribbean, where, however, these zones are wider and boulders are distributed further inland (Scheffers 2002, Watt et al. 2010, Engel & May 2012). The width of the barren zone and the inland distribution of boulders are a function of site-specific Z/H_s values during recurring storm events, which are smaller on Bonaire compared to the study sites in Cuba.

Both, recent examples and the morphologies of older boulders, e.g. at Caleta, indicate that the cliff edge is the primary source of boulders at all three sites, which is in accordance with observations from cliff tops worldwide (Fichaut & Suanez 2011, Paris et al. 2011, Engel & May 2012, Kennedy et al. 2017, Kelletat et al. 2020, Lau & Autret 2020, Pedoja et al. 2023). After quarrying, boulders are either transported inland for short distances (e.g. Baiti 1), or follow gravitational forces and drop into the sea (cf. Kelletat et al. 2020). At Baitiquirí and Majayara, the latter seems to be the predominant process given the high abundance of fresh erosional scars and the low number of cliff-top boulders.

6.2 Boulder transport during Hurricane Matthew compared to global CBD

The sliding transport of Boma 1 (a-axis=10.9 m) for 38 m on top of the elevated carbonate platform is an exceptional observation. The transport of large boulders during storms usually occurs stepwise, usually less than 20 m during one event (e.g., Goto et al. 2009, Boesl et al. 2020), especially at elevations several meters above high tide on a rough, highly karstified surface. Such large transport distances of comparably large boulders during a single storm event have been reported from the Aran Islands in the northeast Atlantic (Cox et al. 2018) or in combination with infragravity waves as in the Philippines (Kennedy et al. 2017), but remain rare. In contrast, during major tsunamis, longer-distance transport of up to several hundreds of meters during a single event is not uncommon (Nandasena et al. 2014, Watanabe et al. 2023). A general pattern of stepwise transport in Cuba up to the general limit of storm transport is also indicated by boulders at Caleta showing several rock pool generations resulting from different resting stages on their way across the coastal platform.

The combination of size and elevation of CBD movement in Cuba during Matthew is at the extreme end compared to datasets of known storm-transported CBD worldwide. Boma 1 plots beyond the corridor defined by the function of Kennedy et al. (2021), but only if the b-axis is considered as the size measure, mostly reflecting a bias introduced by boulder shape. This shows that the function is very sensitive to boulder size, which is not yet satisfactorily accounted for in the dimensionless framework, while the essential other factors of shape (Oetjen et al. 2020), variable fluid density (Nandasena &

Tanaka 2013) or landward distance are not yet considered at all. This also applies to factors such as bottom roughness, transport mode, turbulence, suspension load in the fluid or the effects of vertical jets created by wave impacts at the cliff edge, the role of which is not yet entirely understood either (Kennedy et al. 2017). Further experimental studies of functional relationships of governing parametres are needed and may lead to improvements in dimensionless analysis of the transport of CBD (e.g., Roberts et al. 2025).

Boulder Cal 6 was not moved during Hurricane Matthews, is located further inland and also plots beyond the delimiting function of Kennedy et al. (2021). This indicates predecessor events impacting Guantánamo since the mid-Holocene, either extreme hurricanes similar to or stronger than Hurricane Matthew, passing close to the site, or prehistoric tsunamis (see also Pedoja et al. 2023), which tend to penetrate further inland and imply higher transport capacity and overall longer boulder transport distances (Goto et al. 2009, 2010, Engel et al. 2016). However, our mapping data at the three sites at this point is too selective and not sufficiently exhaustive in order to reliably discuss spatial patterns of tsunami and storm-built boulder fields. Furthermore, it needs to be considered that if the boulder transport is older on time scales of millennia, waves would need to be even more forceful due to a lower RSL (Khan et al. 2017) and, thus, a larger vertical distance Z.

6.3 Predecessor events: Storms or tsunamis?

Given the devastating effects of the event of 2016, hurricanes of similar magnitude or higher intensity occurring at recurrence intervals of 100–500 years in the past (cf. Elsner et al. 2008) and making landfall in southeastern Cuba are the most straightforward interpretation. Lagoonal sediment records from the survey area in southeastern Cuba indicate stronger hurricane activity during the last 2600 years compared to preceding phases, in particular at c. 2600–1800 cal yr. BP and 500–250 cal yr. BP (Peros et al. 2015), supported by overlapping data from Puerto Rico (Donnelly & Woodruff 2007). However, the impact of a major tsunami in the past cannot be excluded to explain the transport of the most landward boulders of up to >100 t, especially for boulder Cal 6 plotting outside the function of eq. 6 (Fig. 9) supposedly delimiting possible transport by storm waves (Kennedy et al. 2021). The only tsunami observations from the south coast of eastern Cuba stem from the city of Santiago de Cuba (Dunán-Avila 2024). In 1755, the town was reportedly "almost completely inundated" from the Lisbon earthquake and tsunami with many buildings damaged inside the bay (NGDC/WDS no year), although this account is associated with uncertainty. A possible impact in Guantánamo Bay, which based on its opening and bathymetry is more exposed towards the Lisbon teletsunami than Santiago de Cuba, remains unclear (Cotilla 2011) and might be a matter of fragmented historical tradition. Another local earthquake in 1775 triggered "waves [causing] extensive destruction". In 1852, "a strong surge in the bay affected the port buildings and loading docks", although there is no information on the cause. At Baracoa, close to the Majayara site, a tsunami of unknown size was reported in August of 1946 (NGDC/WDS no year).

Despite only moderate tsunami impacts reported in historical times, there is a significant hazard of regional tsunamis across longer time frames, e.g. through oblique convergence at the tip of the strike-slip faults along the northern margin of the Caribbean Plate (Fig. 1). This hazard prevails in particular near Hispaniola and Puerto Rico (Calais et al. 1998, Harbitz et al. 2012, Rodríguez-Zurrunero et al. 2019) and as far west as southeastern Cuba (McCann 2006) and the Cayman Trough, where on 08 February 2025 a M7.6 earthquake (Fig. 1) resulted in a tsunami warning of 1–3 m height at the southeastern coast of Cuba (NWS PTWC 2025), which was later lifted. These earthquakes may in addition result in submarine tsunami-triggering mass-wasting events (Grindlay et al. 2005, Rodríguez-Zurrunero et al. 2019).

6.4 Hazard implications in a changing climate

The intensity of hurricanes in the Caribbean is expected to increase until 2100 with moderate confidence under the influence of anthropogenic global warming (Seneviratne et al. 2021). They are fuelled by rising sea surface temperatures (SST) of 2–3 °C between the 1976–2005 and 2071–2100 periods under the representative concentration pathway RCP8.5 where global emissions continue to increase until the end of the century (Bustos & Torres 2021). In addition, Atlantic hurricane systems are slowing down overall under these conditions and will extend the average duration time of

the impact and, thus, extend coastal storm surge (Kossin 2018, Kossin et al. 2020, Vosper et al. 2020, Seneviratne et al. 2021). While Saunders & Lea (2008) found that an SST increase of 0.5 °C in August–September may result in a 40% increase in the frequency of hurricanes, a more recent synthetic assessment of model projections predicts only a slight increase in the frequency of hurricanes of the highest categories 4 and 5 on the Saffir-Simpson scale for the North Atlantic basin (Knutson et al. 2020).

All these findings, in combination with rising RSL, lead to higher inundation levels onshore during storm conditions (Knutson et al. 2020). Despite the fact that the effects of a future poleward shift of hurricane tracks are difficult to assess (Seneviratne et al. 2021), the available projections imply that flood-prone zones indicated by CBD and the landward ramparts should be considered as a minimum indication for setbacks in coastal hazard management across the province of Guantánamo on elevated carbonate platforms – in low-lying coastal areas, the flooding hazard is much greater and needs to be evaluated separately.

7 Conclusions

Coastal boulder movement at the coast of Guantánamo during the passage of hurricane Matthew, which has been exceptional in this region on historical time scales, reflects some typical patterns observed at comparable coastal sites worldwide. These include a boulder source at the cliff edge, preferential sourcing and clustering at shoreline indentations and a stepwise movement of boulder inland across multiple flooding events. The largest boulders experienced sliding transport only, despite the high bottom roughness of the karstified surface. To what extent the high concentration of sand, shells and coral debris in the fluid (Caleta, Baitiquirí) lowered the bottom roughness (as bedload) and increased fluid density and transport capacity (as suspended load) remains open – this also applies to the role of boulder-boulder collision. Some field observations otherwise rarely reported in literature include the high proportion of boulders sourced at the cliff edge during the hurricane and ending up in the shoreface. A more detailed mapping of all boulders at the surveyed sites is needed, however, to more accurately evaluate spatial patterns and reconstruct processes and time frames.

Intense karstification observed in the largest boulders far inland, which were not moved during Hurricane Matthew, indicates an age on centennial or even millennial time scales. These unmoved boulders show that despite the relatively low storminess across Guantánamo in historical times, flooding events even more intense as Hurricane Matthew have occurred in the past, at a very low frequency. Whether these were exceptional hurricanes or tsunamis cannot be determined at this point. However, under current scenarios of climate change flood-prone zones indicated by CBD including the landward ramparts should be considered only as a minimum indication for setbacks in coastal hazard management across the province of Guantánamo.

The dimensionless relationship between size and elevation of the largest boulders moved during Hurricane Matthews and the wave heights measured during the event compares with some of the most extreme patterns of boulder movement of the global dataset used by Kennedy et al. (2021). The boulders from this study plotting close to the limit of possible boulder movement by storm waves support the approach of dimensionless analysis (Kennedy et al. 2021), but also show that it is very sensitive towards inaccurate or variable size measures. Boulder Cal 6 plotting outside this curve in different size-measure scenarios may hint to tsunami deposition in the Holocene past.

Acknowledgements

The reconnaissance survey along the coast of Guantánamo was funded through a Mobility Grant for National and International Young Faculty of the University of Cologne awarded to M.E. Research permits were kindly issued by the Cuban Center of Inspection and Environmental Control (Centro de Inspección y Control Ambiental, CICA). We are thankful for the comments of Serge Suanez, Christine Authemayou, Pedro Luis Dunán-Avila and one anonymous reviewer which greatly improved the original submission.

Data availability

All field data used from the survey are given in Tab. 1. Data was also added to the ISROC database for coastal boulder deposits (Kennedy et al. 2025), accessible through https://doi.org/10.17603/ds2-nm6q-h553, using the ISROC data protocol.

References

Accensi M, Maisondieu C (2015) HOMERE dataset. IFREMER. https://doi.org/10.12770/cf47e08d-1455-4254-955e-d66225c9dc90

Andrews AJ (2007) Spatial and temporal variability of tropical storm and hurricane strikes in the Bahamas, and the Greater and Lesser Antilles. Master's thesis, Louisiana State University. https://doi.org/10.31390/gradschool_theses.3558

Atwater BF, ten Brink US, Cescon AL, Feuillet N, Fuentes Z, Halley RB, Nuñez C, Reinhardt EG, Roger JH, Sawai Y, Spiske M, Tuttle MP, Wei Y, Weil-Accardo J (2017) Extreme waves in the British Virgin Islands during the last centuries before 1500 CE. *Geosphere* 13: 301–368. https://doi.org/10.1130/GES01356.1

Autret R, Dodet G, Fichaut B, Suanez S, David L, Leckler F, Ardhuin F, Ammann J, Grandjean P, Allemand P, Filipot J-F (2016) A comprehensive hydro-geomorphic study of cliff-top storm deposits on Banneg Island during winter 2013–2014. *Marine Geology* 382: 37–55. https://doi.org/10.1016/j.margeo.2016.09.014

Autret R, Dodet G, Suanez S, Roudat G, Fichaut B (2018) Long-term variability of supratidal coastal boulder activation in Brittany (France). *Geomorphology* 304: 184–200. https://doi.org/10.1016/j.geomorph.2017.12.028

Beltrán-Fonseca B (2019) Huracanolitos en Baitiquirí (Guantánamo), movidos por el huracán Matthew: análisis del proceso físico. Aplicación en estudios de paleodeposiciones. Diploma thesis, Universidad Central "Marta Abreu" de Las Villas. https://dspace.uclv.edu.cu/items/dbe9559c-ed6c-4e95-82c6-dcadf0194599 (last access: 12 Dec 2024).

Boesl F, Engel M, Eco RC, Galang JA, Gonzalo LA, Llanes F, Quix E, Brückner H (2020) Digital mapping of coastal boulders – High-resolution data acquisition to infer past and recent transport dynamics. *Sedimentology* 67: 1393–1410. https://doi.org/10.1111/sed.12578

Boudiere E, Maisondieu C, Ardhuin F, Accensi M, Pineau-Gillou L, Lepesqueur J (2013) A suitable metocean hindcast database for the design of marine energy converters. *International Journal of Marine Energy* 3–4: e40–e52. https://doi.org/10.1016/j.ijome.2013.11.010

Bustos Usta DF, Torres Parra RR (2021) Ocean and atmosphere changes in the Caribbean Sea during the twenty-first century using CMIP5 models. *Ocean Dynamics* 71: 757–777. https://doi.org/10.1007/s10236-021-01462-z

Calais E, Perrot J, Mercier de Lepinay B (1998) Strike-slip tectonics and seismicity along the northern Caribbean plate boundary from Cuba to Hispaniola. *Geological Society of America Special Paper* 326: 125–141. https://doi.org/10.1130/0-8137-2326-4.125

CHRR/CIESIN (Center for Hazards and Risk Research, Columbia University/Center for International Earth Science Information Network, Columbia University) (2005) Global Earthquake Hazard Frequency and Distribution (dataset version 1.00). Palisades, NY: NASA Socioeconomic Data and Applications Center (SEDAC). https://doi.org/10.7927/H4765C7S

Clancy C, O'Sullivan J, Sweenet C, Dias F, Parnell AC (2016) Spatial Bayesian hierarchical modelling of extreme sea states. *Ocean Modelling* 107: 1–13. https://doi.org/10.1016/j.ocemod.2016.09.015

Cotilla MO (2011) ¿Tsunamis en Cuba? *Física de la Tierra* 23: 173–197.

Cox R, Jahn KL, Watkins OG, Cox P (2018) Extraordinary boulder transport by storm waves (west of Ireland, winter 2013–2014), and criteria for analysing coastal boulder deposits. *Earth-Science Reviews* 177: 623–636. https://doi.org/10.1016/j.earscirev.2017.12.014

Cox R, Ardhuin F, Dias F, Autret R, Beisiegel N, Earlie CS, Herterich JG, Kennedy A, Paris R, Raby A, Schmitt P (2020) Systematic review shows that work done by storm waves can be misinterpreted as tsunami-related because commonly used hydrodynamic equations are flawed. *Frontiers in Marine Science* 7: 4. https://doi.org/10.3389/fmars.2020.00004

De Beurs KM, McThompson NS, Owsley BC, Henebry GM (2019) Hurricane damage detection on four major Caribbean islands. *Remote Sensing of the Environment* 229: 1–13. https://doi.org/10.1016/j.rse.2019.04.028

De Leeuw G, Neele FP, Hill M, Smith MH, Vignati E (2000) Production of sea spray aerosol in the surf zone. *Journal of Geophysical Research: Atmospheres* 105(D24): 29397–29409. https://doi.org/10.1029/2000JD900549

Donnelly JP, Woodruff JD (2007) Intense hurricane activity over the past 5,000 years controlled by El Niño and the West African Monsoon. *Nature* 447: 465–468. https://doi.org/10.1038/nature05834

Dunán-Avila P (2024) Study of coastal erosion associated with emerging reefs facing cyclones, tsunamis and land/sea interface processes. PhD Thesis, Université de Bretagne Occidentale.

Dunán-Avila P, Authemayou C, Jaud M, Pedoja K, Jara-Muñoz J, Bertin S, Peñalver-Hernández L, Floc'h F, Nuñez-Labañino A, Winckler P, Pierre-Toledo J, Benítez-Frometa P, Ross-Cabrera H, Letortu P, Rodríguez-Valdés AR, Coutín-Lobaina N, Chauveau D (2025) Geomorphological signatures of known hurricanes and validation of theoretical emplacement formulations: Coastal boulder deposits on Cuban low-lying marine terraces. *Marine Geology* 480: 107438. https://doi.org/10.1016/j.margeo.2024.107438

Elsner JB, Jagger TH, Liu K-B (2008) Comparison of hurricane return levels using historical and geological

records. *Journal of Applied Meteorology and Climatology* 47: 368–374. https://doi.org/10.1175/2006JAMC1289.1

Emanuel K (2005) Increasing destructiveness of tropical cyclones over the past 30 years. *Nature* 436:686–688. https://doi.org/10.1038/nature03906

Engel M, May SM (2012) Bonaire's boulder fields revisited: Evidence for Holocene tsunami impact on the Leeward Antilles. *Quaternary Science Reviews* 54: 126–141. https://doi.org/10.1016/j.quascirev.2011.12.011.

Engel M, Oetjen J, May SM, Brückner H (2016) Tsunami deposits of the Caribbean – towards an improved coastal hazard assessment. *Earth-Science Reviews* 163: 260–296. https://doi.org/10.1016/j.earscirev.2016.10.010S

Estrada RE, Morales GM, Hernández-Albernas J, Borrego Acevedo R, Acosta JO, Betancourt YC, Martínez IA, de la Fuente LC (2023) Physical-geographic characteristics of Cuban reefs. Zlatarski VN, Reed JK, Pomponi A, Brooke S, Farrington S (eds) *Coral Reefs of Cuba:* 51–73. Cham. https://doi.org/10.1007/978-3-031-36719-9_3

Fichaut B, Suanez S (2011) Quarrying, transport and deposition of cliff-top storm deposits during extreme events: Banneg Island, Brittany. *Marine Geology* 283: 36–55. https://doi.org/10.1016/j.margeo.2010.11.003

Focke JW (1978) Limestone cliff morphology on Curaçao (Neth. Ant.) with special attention to the origin of notches and vermetid/coralline algal surf benches ('cornices', 'trottoirs'). *Zeitschrift für Geomorphologie N.F.* 22: 329–349.

Gienko GA, Terry JP (2014) Three-dimensional modeling of coastal boulders using multi-view image measurements. *Earth Surface Processes and Landforms* 38: 853–864. https://doi.org/10.1002/esp.3485

Gischler E, Lomando AJ (1997) Holocene cemented beach deposits in Belize. *Sedimentary Geology* 110: 277–297. https://doi.org/10.1016/S0037-0738(96)00088-7

Gómez JF, Cordobés JM, Peña A, Perigó E, Laborde N, Mesa AM, Hernández C, Peña R, Brizuela CM, Beltrán L, Alvarez E (2011) Estudios de peligro, vulnerabilidad y riesgos de desastres de inundación por penetración del mar, inundación por intensas lluvias y afectaciones por fuertes vientos en la provincia Guantánamo. CITMA Guantánamo, scientific report.

Goto K, Miyagi K, Kawamata H, Imamura F (2010) Discrimination of boulders deposited by tsunamis and storm waves at Ishigaki Island, Japan. *Marine Geology* 269: 34–45. https://doi.org/10.1016/j.margeo.2009.12.004

Goto K, Miyagi K, Kawana T, Takahashi J, Imamura F (2011) Emplacement and movement of boulders by known storm waves - field evidence from the Okinawa Islands, Japan. *Marine Geology* 283: 66–78. https://doi.org/10.1016/j.margeo.2010.09.007

Goto K, Okada K, Imamura F (2009) Characteristics and hydrodynamics of boulders transported by storm waves at Kudaka Island, Japan. *Marine Geology* 262: 14–24. https://doi.org/10.1016/j.margeo.2009.03.001

Grindlay NR, Hearne M, Mann P (2005) High risk of tsunami in the northern Caribbean. *Eos* 86: 121–126. https://doi.org/10.1029/2005EO120001

Harbitz CB, Glimsdal S, Bazin S, Zamora N, Løvholt F, Bungum H, Smebye H, Gauer P, Kjekstad O (2012) Tsunami hazard in the Caribbean: regional exposure derived from credible worst case scenarios. *Continental Shelf Research* 38: 1–23. https://doi.org/10.1016/j.csr.2012.02.006

Iturralde-Vinent MA (2017) Huracanolitos, eventos de oleaje extremo y protección de las obras costeras. *Anales de la Academia de Ciencias de Cuba* 7: 4–10.

Jones B, Hunter IG (1992) Very large boulders on the coast of Grand Cayman: The effects of giant waves on rocky coastlines. *Journal of Coastal Research* 8: 763–774.

Kelletat D (2006) Beachrock as sea-level indicator? Remarks from a geomorphological point of view. *Journal of Coastal Research* 22: 1558–1564. https://doi.org/10.2112/04-0328.1

Kelletat D, Scheffers A, Scheffers S (2004) Holocene tsunami deposits on the Bahaman Islands of Long Island and Eleuthera. *Zeitschrift für Geomorphologie N.F.* 48: 519–540. https://doi.org/10.1127/zfg/48/2004/519

Kelletat D, Engel M, May SM, Erdmann W, Scheffers A, Brückner H (2020) Erosive impact of tsunami and storm waves on rocky coasts and post-depositional weathering of coarse-clast deposits. Engel M, Pilarczyk J, May SM, Brill D, Garrett E (eds) *Geological records of tsunamis and other extreme waves:* 561–584. Elsevier, Amsterdam. https://doi.org/10.1016/B978-0-12-815686-5.00028-6

Kelman I (2013) Saffir–Simpson hurricane intensity scale. Bobrowsky PT (ed.) *Encyclopedia of natural hazards:* 882–883. Dordrecht. https://doi.org/10.1007/978-1-4020-4399-4_306

Kennedy AB, Mori N, Yasuda T, Shimozono T, Tomiczek T, Donahue A, Shimura T, Imai Y (2017) Extreme block and boulder transport along a cliffed coastline (Calicoan Island, Philippines) during Super Typhoon Haiyan. *Marine Geology* 383: 65–77. https://doi.org/10.1016/j.margeo.2016.11.004

Kennedy AB, Cox R, Dias F (2021) Storm waves may be the source of some "tsunami" coastal boulder deposits. *Geophysical Research Letters* 48: e2020GL090775. https://doi.org/10.1029/2020GL090775

Kennedy A, Cox R, Engel M, Speyrer E, Lau A, Mori N (2025) The inundation signatures on rocky coastlines global database for coastal boulder deposits (ISROC-DB). *Marine Geology* 487: 107581. https://doi.org/10.1016/j.margeo.2025.107581

Khan NS, Ashe E, Horton BP, Dutton A, Kopp RE, Brocard G, Engelhart SE, Hill DF, Peltier WR, Vane CH, Scatena FN (2017) Drivers of Holocene sea-level change in the Caribbean. *Quaternary Science Reviews* 155: 13–36. https://doi.org/10.1016/j.quascirev.2016.08.032

Kjerfve B (1981) Tides of the Caribbean Sea. *Journal of Geophysical Research* 86(C5): 4243–4247. https://doi.org/10.1029/JC086iC05p04243

Klotzbach PJ (2017): Record-setting North Atlantic hurricane Matthew. *Bulletin of the American Meteorological Society* 98: S106–S107.

Knutson T, Camargo SJ, Chan JCL, Emanuel K, Ho C-H, Kossin J, Mohapatra M, Satoh M, Sugi M, Walsh K, Wu L (2020) Tropical cyclones and climate change assessment – Part II: Projected response to anthropogenic warming. *Bulletin of the American Meteorological Society* 101: E303–E322. https://doi.org/10.1175/BAMS-D-18-0194.1

Kossin JP (2018) A global slowdown of tropical-cyclone translation speed. *Nature* 558: 104–107. https://doi.org/10.1038/s41586-018-0158-3

Kossin JP, Knapp KR, Olander TL, Velden CS (2020) Global increase in major tropical cyclone exceedance probability over the past four decades. *Proceedings of the National Academy of Sciences* 117: 11975–11980. https://doi.org/10.1073/pnas.1920849117

Landsea CW, Franklin JL (2013) Atlantic hurricane database uncertainty and presentation of a new database format. *Monthly Weather Review* 141: 3576–3592. https://doi.org/10.1175/MWR-D-12-00254.1

Lau AYA, Autret R (2020) Spatial patterns of subaerial coarse clasts. Engel M, Pilarczyk J, May SM, Brill D, Garrett E (eds) *Geological records of tsunamis and other extreme waves:* 513–546. Amsterdam. https://doi.org/10.1016/B978-0-12-815686-5.00024-9

Lau AYA, Terry JP, Ziegler A, Pratap A, Harris D (2018) Boulder emplacement and remobilisation by cyclone and submarine landslide tsunami waves near Suva City, Fiji. *Sedimentary Geology* 364: 242–257. https://doi.org/10.1016/j.sedgeo.2017.12.017

Mann ME, Woodruff JD, Donnelly JP, Zhang Z (2009) Atlantic hurricanes and climate over the past 1,500 years. *Nature* 460: 880–883. https://doi.org/10.1038/nature08219

Matos Pupo F, Pérez-López OE, Valero-Jorge A (2022) Hurricane related coastal flooding in the province of Ciego de Avila, Cuba: hazard, vulnerability and risk study. Cardenas R, Mochalov V, Parra O, Martin O (eds.) *Proceedings of the 3rd International Conference on BioGeoSciences:* 105–122. Springer, Cham. https://doi.org/10.1007/978-3-030-88919-7_9

Matos Pupo F, Peros MC, González-De Zayas R, Valero-Jorge A, Pérez-López OE, Álvarez-Taboada F, Sorí R (2023a) Coastal flooding associated with Hurricane Irma in Central Cuba (Ciego de Ávila province). *Atmosphere* 14: 1445. https://doi.org/10.3390/atmos14091445

Matos Pupo F, León-Brito A, Seco-Hernández R, Peros MC (2023b) Distribución espacial de huracanolitos en las costas de Cuba. *Minería y Geología* 39: 1–14.

May SM, Engel M, Brill D, Squire P, Scheffers A, Kelletat D (2013) Coastal hazards from tropical cyclones and extratropical winter storms based on Holocene storm chronologies. Finkl C (ed) *Coastal Hazards:* 557–585. Springer, Dordrecht. https://doi.org/10.1007/978-94-007-5234-4_20.a

May SM, Engel M, Brill D, Cuadra C, Lagmay AMF, Santiago J, Suarez K, Reyes M, Brückner H (2015) Block and boulder transport in Eastern Samar (Philippines) during Supertyphoon Haiyan. *Earth Surface Dynamics* 3: 543–558. https://doi.org/10.5194/esurf-3-543-2015

McCann WR (2006) Estimating the threat of tsunamigenic earthquakes and earthquake induced-landslide tsunami in the Caribbean. Mercado-Irizarry A, Liu P (eds) *Caribbean tsunami hazard:* 43–65. Singapore. https://doi.org/10.1142/9789812774613_0002

Miller S, Rowe D-A, Brown L, Mandal A (2014) Wave-emplaced boulders: Implications for development of "prime real estate" seafront, north coast Jamaica. *Bulletin of Engineering Geology and the Environment* 73: 109–122. https://doi.org/10.1007/s10064-013-0517-0

Mitrani Arenal I (2006) Las inundaciones costeras en Cuba y su repercusión social. *Revista Cubana de Bioética* 6: 1–8.

Mori N, Kato M, Kim S, Mase H, Shibutani Y, Takemi T, Tsuboki K, Yasuda T (2014). Local amplification of storm surge by Super Typhoon Haiyan in Leyte Gulf. *Geophysical Research Letters* 41: 5106–5113. https://doi.org/10.1002/2014GL060689

Muhs DR, Schweig ES, Simmons KR, Halley RB (2017) Late Quaternary uplift along the North America-Caribbean plate boundary: Evidence from the sea level record of Guantanamo Bay, Cuba. *Quaternary Science Reviews* 178: 54–76. https://doi.org/10.1016/j.quascirev.2017.10.024

Muller J, Collins JM, Gibson S, Paxton L (2017) Recent advances in the emerging field of paleotempestology. Collins J, Walsh K (eds) *Hurricanes and Climate Change:* 1–33. Cham. https://doi.org/10.1007/978-3-319-47594-3_1

Mycoo MA (2018) Beyond 1.5 °C: Vulnerabilities and adaptation strategies for Caribbean Small Island Developing States. *Regional Environmental Change* 18: 2341–2353. https://doi.org/10.1007/s10113-017-1248-8

Nandasena NAK (2020) Perspective of incipient motion formulas: Boulder transport by high-energy waves. Engel M, Pilarczyk J, May SM, Brill D, Garrett E (eds) *Geological records of tsunamis and other extreme waves:*

641–659. Amsterdam. https://doi.org/10.1016/B978-0-12-815686-5.00029-8

Nandasena NAK, Tanaka N (2013) Boulder transport by high energy: Numerical model-fitting experimental observations. *Ocean Engineering* 57: 163–179. https://doi.org/10.1016/j.oceaneng.2012.09.012

Nandasena NAK, Tanaka N, Sasaki Y, Osada, M (2014) Reprint of "Boulder transport by the 2011 Great East Japan tsunami: Comprehensive field observations and whither model predictions?". *Marine Geology* 358: 49–66. https://doi.org/10.1016/j.margeo.2014.10.003

Nandasena NAK, Scicchitano G, Scardino G, Milella M, Piscitelli A, Mastronuzzi G (2022) Boulder displacements along rocky coasts: A new deterministic and theoretical approach to improve incipient motion formulas. *Geomorphology* 407: 108217. https://doi.org/10.1016/j.geomorph.2022.108217

NGDC/WDS (National Geophysical Data Center/World Data Service) (no year) NCEI/WDS Global Historical Tsunami Database. NOAA National Centers for Environmental Information. https://doi.org/10.7289/V5PN93H7

Nott J (1997) Extremely high-energy wave deposits inside the Great Barrier Reef, Australia: Determining the cause—tsunami or tropical cyclone. *Marine Geology* 141: 193–207. https://doi.org/10.1016/S0025-3227(97)00063-7

NWS PTWC (National Weather Service Pacific Tsunami Warning Center Honolulu HI) (2025) 0024 UTC Sun Feb 9 2025 Tsunami Message Number 3. https://www.tsunami.gov/events/PHEB/2025/02/08/25039000/3/WECA41/WECA41.txt (last access: 11 February 2025).

Oetjen J, Engel M, Pudasaini SP, Schüttrumpf H (2020) Significance of boulder shape, shoreline configuration and pre-transport setting for the transport of boulders by tsunamis. *Earth Surface Processes and Landforms* 45: 2118–2133. https://doi.org/10.1002/esp.4870.

Otvos EG (2000) Beach ridges—definitions and significance. *Geomorphology* 32: 83–108. https://doi.org/10.1016/S0169-555X(99)00075-6

Paris R, Naylor LA, Stephenson WJ (2011) Boulders as a signature of storms on rock coasts. *Marine Geology* 283: 1–11. https://doi.org/10.1016/j.margeo.2011.03.016

Pedoja K, Dunán-Avila P, Jara-Muñoz J, Authemayou C, Nuñez-Labañino A, De Gelder G, Chauveau D, Peñalver L, De Jesus Benitez Frometa P, Martin-Izquierdo D, Castellanos Abella E, Bertin S, Rodríguez-Valdés ÁR, Arango-Arias ED, Traoré K, Regard, V (2023) On a ~210 t Caribbean coastal boulder: The huracanolito seaward of the ruins of the Bucanero resort, Juragua, Oriente, Cuba. *Earth Surface Processes and Landforms* 48: 3074–3090. https://doi.org/10.1002/esp.5682

Peñalver LL, Denis R, Núñez A, Pérez C, Martín D, Rodríguez L (2013) Nuevos datos sobre los camellones de tormenta en Cuba. Memorias X Congreso de Geología, La Habana 2013, Geo1-P6. http://www.redciencia.cu/geobiblio/paper/2013_Penalver_GEO1-P6.pdf (last access: 06 Feb 2025)

Pérez O, Milanés C (2020) Social perception of coastal risk in the face of hurricanes in the southeastern region of Cuba. *Ocean & Coastal Management* 184: 105010. https://doi.org/10.1016/j.ocecoaman.2019.105010

Pérez R, Vega Y, Limia, M (2001) Los huracanes más intensos y desastrosos de Cuba en los últimos dos siglos. *Boletín de la Sociedad Meteorológica de Cuba* 7: 3-1.

Perigó E, Laborde N, Machado A, Soler Y, Rojas Y, Suárez Bustamante R (2020) Inundaciones costeras en Guantánamo. *Revista Cubana de Meteorología* 26: 1–12.

Peros MC, Gregory B, Matos F, Reinhardt E, Desloges J (2015) Late-Holocene record of lagoon evolution, climate change, and hurricane activity from southeastern Cuba. *The Holocene* 25: 1483–1497. https://doi.org/10.1177/0959683615585844

Reading AJ (1990) Caribbean tropical storm activity over the past four centuries. *International Journal of Climatology* 10: 365–376. https://doi.org/10.1002/joc.3370100404

Roberts S, Raby A, Boulton SJ, Allsop W, Antonini A, Van Balen I, Mcgovern D, Adams K, Chandler I, Cels J, Manzella I (2025) Tsunami boulder transport in coastal environments: Insights from physical experiments and dimensional analysis. *Marine Geology* 481: 107474. https://doi.org/10.1016/j.margeo.2024.107474

Rodríguez A, Acosta E (2017) Megabloques en Trinidad: Generalidades de su morfometría. *Serie Oceanológica* 16: 1–7.

Rodríguez-Zurrunero A, Granja-Bruña JL, Carbó-Gorosabel A, Muñoz-Martín A, Gorosabel-Araus JM, de la Peña LG, Ballesteros MG, Pazos A, Catalán M, Espinosa S, Druet M (2019) Submarine morpho-structure and active processes along the North American-Caribbean plate boundary (Dominican Republic sector). *Marine Geology* 407: 121–147. https://doi.org/10.1016/j.margeo.2018.10.010

Rojas-Consuegra R, Isaac-Mengana J, Matos Pupo F, Peros MC (2019) Coarse detrital deposits from Hurricane Wilma on the western coast of Cojimar, Havana, Cuba. Cárdenas R, Mochalov V, Parra O, Martin O (eds) *Proceedings of the 2nd International Conference on BioGeoSciences:* 111–125. Springer, Cham. https://doi.org/10.1007/978-3-030-04233-2_10

Roura-Pérez P, Sistachs-Vega V, Vega R, Alpizar-Tirzo M (2018) Caracterización estadística climatológica de huracanes en Cuba durante el período 1791–2016. *Revista Cubana de Meteorología* 24: 304–312.

Rovere A, Casella E, Harris DL, Lorscheid T, Nandasena NAK, Dyer B, Sandstrom MR, Stocchi P, D'Andrea WJ, Raymo ME (2017) Giant boulders and Last Interglacial storm intensity in the North Atlan-

tic. *Proceedings of the National Acadademy of Sciences of the U.S.A.* 114: 12144–12149. https://doi.org/10.1073/pnas.1712433114

Saunders M, Lea A (2008) Large contribution of sea surface warming to recent increase in Atlantic hurricane activity. *Nature* 451: 557–560. https://doi.org/10.1038/nature06422

Scheffers A (2002) Paleotsunami in the Caribbean: Field evidences and datings from Aruba, Curaçao and Bonaire. *Essener Geographische Arbeiten* 33. Essen.

Seneviratne SI, Zhang X, Adnan M, Badi W, Dereczynski C, Di Luca A, Ghosh S, Iskandar I, Kossin J, Lewis S, Otto F, Pinto I, Satoh M, Vicente-Serrano SM, Wehner M, Zhou B (2021) Weather and climate extreme events in a changing climate. Masson-Delmotte V, Zhai P, Pirani A, Connors SL, Péan C, Berger S, Caud N, Chen Y, Goldfarb L, Gomis MI, Huang M, Leitzell K, Lonnoy E, Matthews JBR, Maycock TK, Waterfield T, Yelekçi O, Yu R, Zhou B (eds) *Climate Change 2021: The physical science basis. Contribution of Working Group I to the Sixth Assessment Report of the Intergovernmental Panel on Climate Change:* 1513–1766. Cambridge and New York. https://doi.org/10.1017/9781009157896.013

Servicio Hidrográfico y Geodésico de la República de Cuba (2003) Derrotero de las costas de Cuba. GEOCUBA and EDIMAR. Agencia de Cartografía Náutica.

Stewart SR (2017) Hurricane Matthew (AL142016). NOAA/NWS National Hurricane Center. https://www.nhc.noaa.gov/data/tcr/AL142016_Matthew.pdf (last access: 04 Feb 2025).

Styron R (2019) Global Earthquake Model – GEMScience-Tools/gem-global-active-faults: First release of 2019 (Version 2019.0). *Zenodo*. http://doi.org/10.5281/zenodo.3376300

Toscano MA, Rodriguez E, Lundberg J (1999) Geologic investigation of the late Pleistocene Jaimanitas Formation: Science and society in Castro's Cuba. Curran HA, Mylroie JE (eds) *Proceedings of the 9th Symposium on the Geology of the Bahamas and Other Carbonate Regions*: 125–142. San Salvador, Bahamas.

Vanselow KA, Kolb M, Fickert T (2007) Destruction and regeneration of terrestrial, littoral and marine ecosystems on the island of Guanaja/Honduras seven years after Hurricane Mitch. *Erdkunde* 61: 358–371. https://doi.org/10.3112/erdkunde.2007.04.06

Vosper EL, Mitchell DM, Emanuel K (2020) Extreme hurricane rainfall affecting the Caribbean mitigated by the Paris agreement goals. *Environmental Research Letters* 15: 104053. https://doi.org/10.1088/1748-9326/ab9794

Watanabe M, Goto K, Roeber V, Kan H, Imamura F (2023) A numerical modeling approach for better differentiation of boulders transported by a tsunami, storm, and storm-induced energetic infragravity waves. *Journal of Geophysical Research: Earth Surface* 128: e2023JF007083. https://doi.org/10.1029/2023JF007083

Watt SG, Jaffe BE, Morton RA, Richmond BM, Gelfenbaum G (2010) Description of extreme-wave deposits on the northern coast of Bonaire, Netherlands Antilles. *USGS Open-File Report* 2010-1180. https://doi.org/10.3133/ofr20101180

Authors

Dr. Max Engel
https://doi.org/0000-0002-2271-4229
max.engel@uni-heidelberg.de
Institute of Geography
Heidelberg University
Im Neuenheimer Feld 348
69120 Heidelberg
Germany

Prof. Dr. Felipe Matos Pupo
https://doi.org/0000-0002-6070-5462
Centro Meteorológico Provincial de Ciego de Ávila
Avenida Los Deportes
Ciego de Ávila
Cuba

Zadiérik Hernández Ortega
https://doi.org/0000-0002-9216-3055
Centro de Aplicaciones Tecnológicas para el Desarrollo Sostenible (CATEDES)
Guantánamo
Cuba

PD Dr. Dominik Brill
https://doi.org/0000-0001-8637-4641
brilld@uni-koeln.de
Institute of Geography
University of Cologne
Otto-Fischer-Str. 4
50674 Cologne
Germany